Inorg. Chem. **2004**, *43*, 5147–5158

Comparative Structural Studies of Iodide Complexes of Uranium(III) and Lanthanide(III) with Hexadentate Tetrapodal Neutral N-Donor Ligands

Lydia Karmazin,[†] Marinella Mazzanti,*[,†] Jean-Philippe Bezombes,[†] Christelle Gateau,[†] and Jacques Pécaut[‡]

Laboratoire de Reconnaissance Ionique and Laboratoire de Coordination et Chiralité, Service de Chimie Inorganique et Biologique, CEA/DSM/Département de Recherche Fondamentale sur la Matière Condensée, CEA-Grenoble, 38054 Grenoble, Cedex 09, France

Received April 8, 2004

The syntheses, the solution structures, and the crystal structures of the two new tetrapodal N-donor ligands *N*,*N*,*N*′,*N*′-tetrakis(2-pyrazylmethyl)-1,3-trimethylenediamine (tpztn), **1**, and *N*,*N*,*N*′,*N*′-tetrakis(2-pyrazylmethyl)-*trans*-1,2-cyclohexanediamine (tpzcn), **2**, are described. Two different geometric isomers of the cation $[La(tpztn)I_2]^+$ were isolated in which the ligand adopts two different conformations leading to strong differences in the metal–ligand bond distances. The crystal structure of isostructural complexes of La, U, Ce, and Nd were determined by X-ray diffraction studies for the ligands tpztn and tpzcn. In both series of complexes the two methylpyrazyl arms and the diamine spacer (trimethylene or cyclohexane) around each aliphatic nitrogen adopt the same helical configuration. The complexes crystallize as a racemic mixture of Λ,Λ and Δ,Δ enantiomers with distorted square antiprism geometries. In these complexes the $M–N_{pyrazine}$ distances show a decrease from La to Ce and from La to Nd which corresponds well to the decrease in ionic radius as expected in a purely ionic bonding model. Conversely the mean value of the $U–N_{pyrazine}$ distances is shorter (0.043(3) Å for tpztn and 0.054(11) Å for tpzcn) than the mean value of the $La–N_{pyrazine}$ distances. These differences are significantly larger than the decrease expected from the variation of the ionic radii and can be interpreted in terms of a stronger M–N interaction for U(III). Previously reported extraction studies have shown that while the tripod tris[(2-pyrazyl)methyl]amine (tpza) containing three pyrazyl nitrogens extracts An(III) preferentially to Ln(III), tpztn and tpzcn display no selectivity despite the presence of four pyrazyl groups connected to a different spacer. The structural studies described here show that despite the lack of selectivity observed in the extraction conditions, the arrangement of pyrazyl nitrogens in the tetrapodal architectures of tpztn and tpzcn allows for metal–ligand interaction similar to that observed for tpza.

Introduction

The design of selective extractants for the separation of trivalent actinides from trivalent lanthanides is one of the key problems in nuclear waste reprocessing.[1−4] Heterocyclic imines have been reported to complex actinides(III) more strongly than lanthanides(III), owing to a greater covalent contribution to the metal−nitrogen bonding. Tridentate ligands such as 2,2′:6,2″-terpyridine (terpy), 2,4,6-tris(4-alkyl-2-pyridyl)-1,3,5-triazine,[5,6] 2,6-bis(5-alkyl-1,2,4-triazol-3-yl)pyridine, and 2,6-bis(5,6-dialkyl-1,2,4-triazine-3-yl)-pyridine (Rbtp),[7,8] tetradentate tripodal oligoamines such as tris[(2-pyridyl)methyl]amine (tpa) and tris[(2-pyrazyl)methyl]-amine (tpza),[9,10] and the hexadentate tetrapodal oligoamine

* Author to whom correspondence should be addressed. E-mail: mazzanti@drfmc.ceng.cea.fr.
† Laboratoire de Reconnaissance Ionique.
‡ Laboratoire de Coordination et Chiralité.

(1) *Actinides and Fission Products Partitioning and Transmutation, Status and Assessment Report*, Proceedings of the 5th OECD/NEA Information Exchange Meeting on Actinide and Fission Product Partitioning and Transmutation, Mol, Belgium, Nov 25−27, 1998; NEA/OECD: Paris, 1999.
(2) Kolarik, Z. *Separation of Actinides and Long-Lived Fission Products from High-level Radioactive Wastes (a review)*; Kernforschungszentrum: Karlsruhe, Germany, 1991.
(3) Jarvinen, G. D. *Chemical Separation Technologies and Related Methods of Nuclear Waste Management*; Kluwer Academic Publishers: Dordrecht, The Netherlands, 1999.
(4) Nash, K. N. *Ion Exch. Solvent Extr.* **1993**, *11*, 729.
(5) Hagstrom, I.; Spjuth, L.; Ernasson, A.; Liljenzin, J. O.; Skalberg, M.; Hudson, M.; Iveson, P. B.; Madic, C.; Cordier, P.-Y.; Hill, C.; François, N. *Ion Exch. Solvent Extr.* **1999**, *17*, 221.
(6) Cordier, P.-Y.; Hill, C.; Baron, P.; Madic, C.; Hudson, M.; Liljenzin, J. O. *J. Alloys Compd.* **1998**, *271*−*273*, 738.
(7) Kolarik, Z.; Müllich, U.; Gassner, F. *Ion Exch. Solvent Extr.* **1999**, *17*, 23.
(8) Kolarik, Z.; Müllich, U.; Gassner, F. *Ion Exch. Solvent Extr.* **1999**, *17*, 1155.

10.1021/ic049538m CCC: $27.50
Published on Web 07/13/2004

N,*N*,*N*′,*N*′-tetrakis(2-pyrazylmethyl)ethylenediamine (tpzen)[11] have been shown to selectively extract actinides in preference to the lanthanides from nitric acid solutions into an organic phase. The An(III)/Ln(III) selectivity observed for these ligands could be explained by a covalent contribution to the $An-N_{aromatic}$ bond leading to a stronger M−N interaction with respect to the essentially electrostatic Ln−N bond. While bonding in f elements is traditionally described as essentially electrostatic, the issue of f covalency has often been subject of debate in the past years.[12−15] The presence of strong metal−ligand back-donation could explain the recently described formation of uranium(III) carbonyl complexes, which appear to violate this predominantly electrostatic description of bonding.[16−19] The analysis of structural data for a large number of complexes[14,20] has been used to evaluate the degree of covalency of metal−ligand bonding in organoactinides. Metal to phosphorus bond lengths in trivalent uranium and trivalent cerium metallocene complexes with phosphine and phosphite ligands have been rationalized by Brennan and co-workers in terms of U(III) to phosphorus π back-bonding and of the lack of π back-bonding in cerium complexes.[21] The comparison of ν_{CN} stretching frequencies in isocyanide complexes of trivalent uranium and trivalent cerium metallocene also shows a better π donating ability of U(III) metallocenes than their Ce(III) analogous.[22] Numerous calculations evaluating the differences in bonding of 5f with respect to 4f elements have also been recently reported.[23−26]

To relate possible structural differences between La(III) and U(III) complexes with the presence of a larger degree of covalency in the $U(III)-N_{aromatic}$ interaction we have compared isostructural complexes of La and U containing the same iodide counterion with the tripodal ligands tpa and tpza.[10,27] The observed structural differences and the density functional studies of the tpza complexes indicate the presence of a U−N π back-bonding interaction. A similar structural study has been done on the tridentate nitrogen ligands terpy and Rbtp, which has also led to the conclusion of the presence of a U−N π back-bonding interaction.[28,29] Moreover a relationship can be established between the magnitude of the differences in $M-N_{aromatic}$ distances between U(III) and Ce(III) or La(III) observed in these studies, the selectivity in An(III)/Ln(III) separation, and the π acceptor character of the ligands (Rbtp > terpy ∼ tpza > tpa). However, other parameters, besides the nature of the donor atoms, can be very important for the enhancement of metal ion binding selectivity.[30] Despite the large number of N-donor extractants studied, the relationship between the architecture linking the donor atoms of the extractant and its selectivity remains unexplored.

We have recently communicated the An(III)/Ln(III) separation properties of three new neutral tetrapodal N-donor ligands containing four methylpyrazyl arms connected to different diamine spacers (ethylenediamine, trimethylenediamine, cyclohexanediamine).[11] Although the donor atoms in these ligands are the same, a drastic difference in selectivity was observed which indicates the existence of a strong correlation between the ligand architecture and the selectivity of metal ion recognition. To elucidate further the coordination properties responsible for these differences we are studying the structural and electronic properties of the U(III) and Ln(III) complexes of these ligands. In this work we investigated if the metal−nitrogen bond distances in their 4f and 5f complexes correlate with the selectivity of these ligands in An(III)/Ln(III) separation as found for tripodal and tridentate ligands. We describe the structural properties in the solid state and in solution of the uranium(III) and lanthanide(III) complexes of the ligand tpztn *N*,*N*,*N*′,*N*′-tetrakis-(2-pyrazylmethyl)-1,3-trimethylenediamine and *N*,*N*,*N*′,*N*′-tetrakis(2-pyrazylmethyl)-*trans*-1,2-cyclohexanediamine-(tpzcn). (see Chart 1). The previously reported extraction studies have shown that while the tripode tpza containing three pyrazyl nitrogens extracts An(III) preferentially to Ln-(III) (10−35 times more), tpztn and tpzcn display no selectivity despite the presence of four pyrazyl groups connected to a different spacer. Here we show that despite the lack of selectivity observed in the extraction conditions, the arrangement of pyrazyl nitrogens in the tetrapodal architectures of tpztn and tpzcn allows for a metal−ligand interaction similar to that observed for tpza.

Experimental Section

General Details. ^{1}H NMR spectra were recorded on Bruker AM-400, Bruker Avance 500, and Varian U-400 spectrometers using $CDCl_3$ and CD_3CN solvents with $CHCl_3$ and CH_3CN as internal standards. CD_3CN was vacuum distilled from CaH_2 after a 48 h reflux. The elemental analyses of the ligands tpztn and tpzcn were

(9) Wietzke, R.; Mazzanti, M.; Latour, J.-M.; Pecaut, J.; Cordier, P.-Y.; Madic, C. *Inorg. Chem.* **1998**, *37*, 6690.
(10) Mazzanti, M.; Wietzke, R.; Pécaut, J.; Latour, J.-M.; Maldivi, P.; Remy, M. *Inorg. Chem.* **2002**, *41*, 2389.
(11) Karmazin, L.; Mazzanti, M.; Gateau, C.; Hill, C.; Pécaut, J. *Chem. Commun.* **2002**, 2892.
(12) Raymond, K. N.; Eigenbrot, C. W., Jr. *Acc. Chem. Res.* **1980**, *13*, 276.
(13) Burns, C. J.; Bursten, B. E. *Comments Inorg. Chem.* **1989**, *9*, 61.
(14) Sockwell, S. C.; Hanusa, T. P. *Inorg. Chem.* **1990**, *29*, 76.
(15) Freedman, D.; Melman, J. H.; Emge, T. J.; Brennan, J. G. *Inorg. Chem.* **1998**, *37*, 4162.
(16) Brennan, J. G.; Andersen, R. A.; Robbins, J. L. *J. Am. Chem. Soc.* **1986**, *108*, 335.
(17) Cloke, F. G. N. *Chem. Soc. Rev.* **1993**, *22*, 17.
(18) Parry, J.; Carmona, E.; Simon, C.; Hursthouse, M. *J. Am. Chem. Soc.* **1995**, *117*, 2649.
(19) Evans, W. J.; Kozimor, S. A.; Nyce, G., W.; Ziller, J. W. *J. Am. Chem. Soc.* **2003**, *125*, 13831.
(20) Brennan, J. G.; Stults, S. D.; Andersen, R. A.; Zalkin, A. *Inorg. Chim. Acta* **1987**, *139*, 201.
(21) Brennan, J. G.; Stults, S. D.; Andersen, R. A.; Zalkin, A. *Organometallics* **1988**, *7*, 1329.
(22) Conejo, M. d. M.; Parry, J. S.; Carmona, E.; Schultz, M.; Brennan, J.; Beshouri, S. M.; Andersen, R. A.; Rogers, R. D.; Coles, S.; Hursthouse, M. *Chem.−Eur. J.* **1999**, *5*, 3000.
(23) Diaconescu, P. L.; Cummins, C. C. *J. Am. Chem. Soc.* **2002**, *124*, 7660.
(24) Jensen, M. P.; Bond, A. H. *J. Am. Chem. Soc.* **2002**, *124*, 7660.
(25) Vetere, V.; Maldivi, P.; Adamo, C. *J. Comput. Chem.* **2003**, *24*, 850.
(26) Kaltsoyannis, N. *Chem. Soc. Rev.* **2003**, *32*, 9.
(27) Wietzke, R.; Mazzanti, M.; Latour, J.-M.; Pécaut, J. *J. Chem. Soc., Dalton Trans.* **2000**, 4167.
(28) Berthet, J.-C.; Miquel, Y.; Iveson, P.; Nierlich, M.; Thuéry, P.; Madic, C.; Ephritikhine, M. *J. Chem. Soc., Dalton Trans.* **2002**, 3265.
(29) Berthet, J.-C.; Rivière, C.; Miquel, Y.; Nierlich, M.; Madic, C.; Ephritikhine, M. *Eur. J. Inorg. Chem.* **2002**, 1439.
(30) Berthet, J.-C.; Nierlich, M.; Ephritikhine, M. *Polyhedron* **2003**, *22*, 3475.

Chart 1

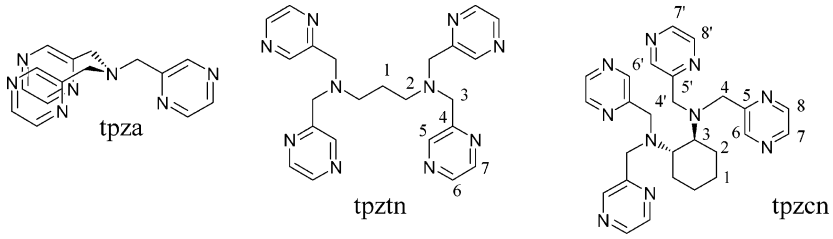

performed by SCA/CNRS, Vernaison, France. Elemental analyses of the complexes were performed under argon by Analytische Laboratorien GmbH at Lindlar, Germany. Mass spectra were obtained with a Finnigan LCQ-ion trap equipped with an electrospray source. Melting points were taken on an Electrothermal IA93000 melting point apparatus and are reported uncorrected. Flash chromatography was performed using silica gel Si 60 (40−63 μm, Merck) or aluminum oxide 90 active neutral (0.063−0.200 mm, Merck).

All manipulations of the lanthanide and uranium complexes were carried out under an inert-argon atmosphere using Schlenk techniques and a Braun glovebox equipped with a purifier unit. The water and oxygen level were always maintained at less than 1 ppm. The solvents were purchased from Aldrich in their anhydrous form, were transferred into a Schlenk flask under argon, and were vacuum distilled from K (diisopropyl ether and tetrahydrofuran) or CaH_2 (acetonitrile). Depleted uranium turnings were purchased from the "Societé Industrielle Combustible Nucleaire" of Annecy, France. Starting materials were purchased from Aldrich, Fluka, and Alfa and used without further purification unless otherwise stated. Anhydrous LnI_3 (Ln = La, Ce, Nd, Lu) were purchased from Aldrich. 2-(Chloromethyl)pyrazine was prepared from the commercially available 2-methylpyrazine according to a modification of the published procedure which replaces the more toxic carbon tetrachloride with chloroform.[31,32]

$[UI_3(thf)_4]$ was prepared as described by Clark and co-workers.[33,34] $[LnI_3(thf)_n]$ (Ln = La, Ce, $n = 4$; Ln = Nd, Lu, $n = 3.5$)[35] were prepared by stirring overnight anhydrous LnI_3 in thf. The white (La, Ce, Lu) or pale blue (Nd) powders obtained after filtration were purified by extraction in hot thf to give microcrystalline solids (80−90% yield).

Synthesis of the Ligands tpztn and tpzcn. 2-(Chloromethyl)-pyrazine. To a solution of 2-methylpyrazine (4.85 mL, 53.1 mmol) in chloroform (180 mL) was added dichlorantine (8.37 g, 42.5 mmol) under an argon atmosphere. The reaction mixture was refluxed for 16 h, and two portions of AIBN (2 × 0.174 g, 2 × 1.06 mmol) were added after 30 min and 2 h. After being cooled at 0 °C, the solution was filtrated and concentrated under vacuum. The resulting crude product (11.5 g) was purified by flash chromatography (600 mL silica gel, 50/50 diethyl ether/petroleum ether) to give 2-(chloromethyl)pyrazine (3.62 g, 53%) as an unstable light yellow oil.

^{1}H NMR ($CDCl_3$, 400 MHz, 298 K, δ): 8.74 (d, $J = 0.9$ Hz, 1H, H_3), 8.56 (m, 2H, H_5/H_6), 4.70 (s, 2H, CH_2Cl).

***N,N,N′,N′*-Tetrakis(2-pyrazylmethyl)-1,3-trimethylenediamine (tpztn), 1.** To a solution of 2-(chloromethyl)pyrazine (3.54 g, 27.6 mmol) in anhydrous acetonitrile (50 mL) were successively added 1,3-propanediamine (0.48 mL, 5.74 mmol), K_2CO_3 (3.81 g, 27.6 mmol), and KI (4.57 g, 27.6 mmol) under an argon atmosphere. The reaction mixture was refluxed for 16 h. After filtration and evaporation of the solvent, the residue was dissolved in CH_2Cl_2 (100 mL) and the organic layer was washed with a saturated aqueous $NaHCO_3$ solution (100 mL). The aqueous layer was then extracted with CH_2Cl_2 (6 × 50 mL). The combined organic layers were dried with Na_2SO_4 and concentrated. The resulting crude product (2.67 g) was purified by flash chromatography (300 mL of aluminum oxide; CH_2Cl_2/MeOH, gradient from 100/0 to 95/5) followed by crystallization in diethyl ether/petroleum ether mixture to give tpztn (1.90 g, 74%) as a beige solid.

Anal. Calcd for $C_{23}H_{26}N_{10}$ ($M_r = 442.52$): C, 62.43; H, 5.92; N, 31.65. Found: C, 62.36; H, 5.95; N, 31.74. Mp: 67−68 °C. ^{1}H NMR ($CDCl_3$, 400 MHz, 298 K, δ): 8.64 (d, $J = 1.4$, 4H, H_5), 8.48 (dd, $J = 2.4, 1.4$, 4H, H_7), 8.43 (d, $J = 2.4$, 4H, H_6), 3.03 (s, 8H, H_3), 2.61 (t, $J = 7.2$, 4H, H_2), 1.84 (quint, $J = 7.2$ Hz, 2H, H_1). ^{1}H NMR (CD_3CN, 400 MHz, 298 K, δ): 8.60 (d, $J = 1.3$, 4H, H_5), 8.43 (dd, $J = 2.5, 1.3$, 4H, H_7), 8.39 (d, $J = 2.5$, 4H, H_6), 3.77 (s, 8H, H_3), 2.55 (t, $J = 7.1$, 4H, H_2), 1.76 (q, $J = 7.1$ Hz, H_1). ^{13}C NMR ($CDCl_3$, 100 MHz, 298 K, δ): 154.8 (C_4), 145.3 (CH_{Ar}), 144.0 (CH_{Ar}), 143.4 (CH_{Ar}), 58.1 (C_3), 52.5 (C_2), 25.0 (C_1). ES-MS: m/z 443.2 ($[M + H]^+$).

Crystals suitable for X-ray diffraction studies were obtained by slow evaporation of a solution of tpztn in acetonitrile.

***N,N,N′,N′*-Tetrakis(2-pyrazylmethyl)-*trans*-1,2-cyclohexanediamine (tpzcn), 2.** To a solution of (±)-*trans*-1,2-diaminocyclohexane (0.71 mL, 5.91 mmol) in anhydrous acetonitrile (30 mL) were successively added 2-(chloromethyl)pyrazine (3.80 g, 29.6 mmol) in anhydrous acetonitrile (20 mL), K_2CO_3 (3.92 g, 28.4 mmol), and KI (4.71 g, 28.4 mmol) under an argon atmosphere. The reaction mixture was refluxed for 16 h. After filtration and evaporation of the solvent, the residue was dissolved in CH_2Cl_2 (200 mL) and the organic layer was washed with a half-saturated aqueous $NaHCO_3$ solution (2 × 200 mL). The aqueous layer was then extracted with CH_2Cl_2 (4 × 100 mL). The combined organic layers were dried with Na_2SO_4 and concentrated. The resulting crude product (3.16 g) was purified by flash chromatography (400 mL of aluminum oxide; CH_2Cl_2/MeOH, gradient from 100/0 to 95/5) followed by crystallization in ethyl acetate to give tpzcn (1.93 g, 68%) as a beige solid.

Anal. Calcd for $C_{26}H_{30}N_{10}$ ($M_r = 482.59$): C, 64.71; H, 6.27; N, 29.02. Found: C, 64.42; H, 6.34; N, 28.68. Mp: 110−111 °C. ^{1}H NMR ($CDCl_3$, 400 MHz, 298 K, δ): 8.71 (d, $J = 1.5$, 4H, H_6), 8.41 (dd, $J = 2.5, 1.5$, 4H, H_8), 8.35 (d, $J = 2.5$, 4H, H_7), 3.76, 3.87 (AB, $J = 14.4$ Hz, 8H, H_4), 2.86 (m, 2H, H_3), 2.17 (m, 2H, H_{1ax}), 1.81 (m, 2H, H_{1eq}), 1.19 (m, 4H, H_2). ^{1}H NMR (CD_3CN, 400 MHz, 298 K, δ): 8.65 (d, $J = 1.5$, 4H, H_6), 8.41 (dd, $J = 2.5, 1.5$, 4H, H_8), 8.3 (d, $J = 2.5$, 4H, H_7), 3.79, 3.70 (AB, $J = 14.4$ Hz, 8H, H_4), 2.89 (m, 2H, H_3), 2.13 (m, 2H, H_{1ax}), 1.77 (m, 2H, H_{1eq}), 1.20 (m, 4H, H_2). ^{13}C NMR ($CDCl_3$, 100 MHz, 298 K, δ): 155.5 (C_5), 146.0 (CH_{Ar}), 143.8 (CH_{Ar}), 143.2 (CH_{Ar}), 61.4 [N*C*H-

(31) Abushanab, E.; Bindra, A. P.; Goodman, L.; Peterson, H., Jr. *J. Org. Chem.* **1973**, *38*, 2049.
(32) Newkome, G. R.; Kiefer, G., E.; Xia, Y.-J.; Gupta, V. K. *Synthesis* **1984**, 676.
(33) Clark, D. L.; Sattelberger, A. P.; Andersen, R. A. *Inorg. Synth.* **1997**, *31*, 307.
(34) Avens, L. R.; Bott, S. G.; Clark, D. L.; Sattelberger, A. P.; Watkin, J. G.; Zwick, B. D. *Inorg. Chem.* **1994**, *33*, 2248.
(35) Izod, K.; Liddle, S. T.; Clegg, W. *Inorg. Chem.* **2004**, *43*, 214.

$(CH_2)_4CHN$], 54.0 (C_4), 25.9, 25.8 [NCH(CH_2)$_4$CHN]. ES-MS: *m*/*z* 483.3 ([M + H]$^+$).

Crystals suitable for X-ray diffraction studies were obtained by slow evaporation of a solution of tpzcn in acetonitrile.

Synthesis of the tpztn Complexes. [La(tpztn)I$_3$]. A solution of $LaI_3(thf)_4$ (78.7 mg, 0.100 mmol) in CH_3CN (1.0 mL) was added to a solution of tpztn (44.2 mg, 0.100 mmol) in CH_3CN (1.5 mL). The resulting yellow solution was left standing for 3 days at room temperature. Bright yellow crystals were then collected, washed with CH_3CN (2 × 1.0 mL), and dried under vacuum (2 h). The filtrate was concentrated to ca. 1.0 mL, yielding a second crop of [La(tpztn)I$_2$]I, **3**, as a bright yellow microcrystalline solid. Combined yield: 67% (63 mg).

Anal. Calcd for [La(tpztn)I$_2$]I, $C_{23}H_{26}I_3N_{10}La$: C, 28.71; H, 2.72; N, 14.56. Found: C, 28.77; H, 2.89; N, 14.74. ^{1}H NMR (500 MHz, CD_3CN, 298 K, δ): 8.98 (s, 4H, H_7), 8.73 (s, 4H, H_5), 8.64 (d, J = 2.5, 4H, H_6), 4.73, 4.20 (AB, J = 16.1, 8H, H_3), 3.22 (t, J = 4.4, 4H, H_2), 2.00 (q, J = 4,4 Hz, 2H, H_1). EI-MS (CH_3CN): *m*/*z* 835 ([La(tpztn)I$_2$]$^+$). Λ_M (CH_3CN, 293 K, C = 10^{-3} M): 189 Ω^{-1-}·cm^2·mol^{-1}.

Crystals of [La(tpztn)I$_2$]I, **3**, suitable for X-ray diffraction studies were obtained by slow diffusion of diisopropyl ether into a 1:1 solution of tpztn and $LaI_3(thf)_4$ in acetonitrile. Crystals of [La(tpztn)I$_2$]I·1.17CH_3CN, **4**, suitable for X-ray diffraction studies were obtained from a 1:1 solution (4.5 × 10^{-2} M) of tpztn and $LaI_3(thf)_4$ in acetonitrile left to stand at room temperature for few days.

[Ce(tpztn)I$_3$]. A solution of $CeI_3(thf)_4$ (81.0 mg, 0.100 mmol) in CH_3CN (2.0 mL) was added to a solution of tpztn (44.3 mg, 0.100 mmol) in CH_3CN (1.0 mL). The resulting bright yellow solution was left to stand for 2 days. Bright yellow crystals were then collected, washed with CH_3CN (2 × 1.0 mL), and dried under vacuum(2 h). Yield: 74% (71 mg).

Anal. Calcd for [Ce(tpztn)I$_2$]I, $C_{23}H_{26}I_3N_{10}Ce$: C, 28.68; H, 2.72; N, 14.54. Found: C, 28.90; H, 2.84; N, 14.70. ^{1}H NMR (400 MHz, CD_3CN, 343 K, δ): 13.74 (br s, 4H), 9.93 (s, 4H), 8.87 (s, 4H), 4.52 (br s, 4H), 3.48 (br s, 4H), 1.13 (br s, 2H), −1.78 (br s, 4H).

Crystals of [Ce(tpztn)I$_2$]I·1.17CH_3CN, **5**, suitable for X-ray diffraction studies were obtained from a 1:1 (1.4 × 10^{-2} M) solution of tpztn and $CeI_3(thf)_4$ in acetonitrile left to stand at room temperature for few days.

[Nd(tpztn)I$_3$]. A pale green solution of $NdI_3(thf)_{3.5}$ (100 mg, 0,123 mmol) in CH_3CN (2.0 mL) was added to a solution of tpztn (54.4 mg, 0,123 mmol) in CH_3CN (2.0 mL). The resulting pale yellow solution was stirred for 10 min at room temperature. After the solution was left standing for a few hours at room temperature, a pale yellow solid formed. After the mixture was filtered, washed with CH_3CN, and dried under vacuum (10 min), 43 mg (85%) of pale yellow microcrystalline solid was collected.

Anal. Calcd for [Nd(tpztn)I$_2$]I·1.17CH_3CN, $C_{25.33}H_{29.50}I_3NdN_{11.17}$: C, 29.96; H, 2.93; N, 15.41. Found: C, 29.94; H, 3.05; N, 15.33. ^{1}H NMR (CD_3CN, 500 MHz, 333 K, δ): 18.05 (s, 4H, H_5), 11.36 (s, 4H, H_6), 9.47 (s, 4H, H_7), 7.44 (s, 4H, H_2), 4.75 (s, 4H, H_{3A}), 0.42 (s, 2H, H_1), −3.3 (v br s, 4H, H_{3B}). Λ_M (CH_3CN, 293 K, C = 10^{-3} M): 183 Ω^{-1}·cm^2·mol^{-1}.

Crystals of [Nd(tpztn)I$_2$]I·1.17CH_3CN, **6**, suitable for X-ray diffraction studies were obtained from a 1:1 (1.4 × 10^{-2} M) solution of tpztn and $NdI_3(thf)_4$ in acetonitrile left to stand at room temperature for few days.

[U(tpztn)I$_3$]. A green solution of $UI_3(thf)_4$ (91.0 mg, 0.100 mmol) in CH_3CN (1.0 mL) was added to a solution of tpztn (44.2 mg, 0.100 mmol) in CH_3CN (1.0 mL). The resulting dark blue solution was left to stand for 1 day. Dark blue crystals were then collected, washed with CH_3CN (2 × 1.0 mL), and dried under vacuum for 2 h. The filtrate was concentrated to ca.. 1.0 mL, and diisopropyl ether (ca. 0.2 mL) was added. After 3 days, a second crop of crystals was collected. Combined yield: 40% (42 mg). Anal. Calcd for [U(tpztn)I$_2$]I, $C_{23}H_{26}I_3N_{10}U$: C, 26.03; H, 2.47; N, 13.20. Found: C, 26.20; H, 2.42; N, 13.38. ^{1}H NMR (500 MHz, CD_3CN, 333 K, δ): 26.01 (s, 4H, H_7), 10.75 (s, 4H, H_5). 9.03 (s, 4H, H_6), −0.80 (s, 4H, H_2), −3.44 (s, 4H, H_{3B}), −5.40 (s, 4H, H_{3A}), −8.52 (s, 2H, H_1).

Crystals of [U(tpztn)I$_2$]I·1.17CH_3CN, **7**, suitable for X-ray diffraction studies were obtained from a 1:1 solution (3.7 × 10^{-2} M) of tpztn and $UI_3(thf)_4$ in acetonitrile left to stand at room temperature for few days.

[Lu(tpztn)I$_3$]. A solution of $LuI_3(thf)_{3.5}$ (42.2 mg, 5.0 × 10^{-2} mmol) in CH_3CN (4.5 mL) was added to a solution of tpztn (20.0 mg, 4.52 × 10^{-2} mmol) in CH_3CN (4.5 mL). After the resulting yellow solution was left standing a few hours at room temperature, bright yellow crystals formed. After filtration, washing with CH_3CN, and drying under vacuum (10 min), 43 mg (85%) of yellow microcrystalline solid was collected.

Anal. Calcd for [Lu(tpztn)(CH_3CN)$_2$]I$_3$.1.5CH_3CN, $C_{30}H_{36.5}I_3LuN_{13.5}$: C, 31.53; H, 3.19; N, 16.55. Found: C, 31.31; H, 3.19; N, 16.77. ^{1}H NMR (400 MHz, CD_3CN, 343 K, δ) of the major species: 9.02 (s, 4H, H_{Ar}), 8.88 (s, 4H, H_{Ar}), 4.30, 4.53 (AB, J = 16.6, H_3), 3.14 (t, J = 4.8 Hz, 4H, H_2),1.34 (m, 2H, H_1). A very broad signal is present in the 8−9 ppm region. ^{1}H NMR (400 MHz, CD_3CN, 238 K, δ) of the major species: 9.32 (s, 2H, H_{Ar}), 9.22 (s, 2H, H_{Ar}), 9.22 (s, 2H, H_{Ar}), 8.97 (s, 2H, H_{Ar}), 8.75 (s, 2H, H_{Ar}), 7.29 (s, 2H, H_{Ar}), 4.17, 4.35 (AB, J = 16.5, H_3), 4.46, 4.54 (AB, J = 16.1, H_3), 3.22 (2H, H_2), 3.17 (2H, H_2), 1.31 (m, 2H, H_1). Λ_M (CH_3CN, 293 K, C = 10^{-3} M): 265 Ω^{-1}·cm^2·mol^{-1}.

Crystals of [Lu(tpztn)(CH_3CN)$_2$]I$_3$·CH_3CN, **8**, suitable for X-ray diffraction studies were obtained from a 1:1 (0.5 × 10^{-2} M) solution of tpztn and $LuI_3(thf)_{3.5}$ in acetonitrile left to stand at room temperature for few days.

Synthesis of the tpzcn Complexes. [La(tpzcn)I$_3$]. A solution of $LaI_3(thf)_4$ (67.0 mg, 0.083 mmol) in CH_3CN (2.0 mL) was added to a solution of tpzcn (40.0 mg, 0.083 mmol) in CH_3CN (2.0 mL). The resulting yellow solution was left to stand for 1 day. A yellow crystalline solid was then collected, washed with CH_3CN (2 × 2.0 mL), and dried under vacuum. Yield: 82% (69.6 mg).

Anal. Calcd for [La(tpzcn)I$_2$]I·0.5CH_3CN, $C_{27}H_{31.5}I_3N_{10.5}La$: C, 31.54; H, 3.09; N, 14.31. Found: C, 31.43; H, 3.29; N, 14.37. ^{1}H NMR (CD_3CN, 500 MHz, 298 K, δ): 9.33 (s, 2H, H_8), 8.94 (s, 2H, H_6), 8.84 (d, J = 2.6, 2H, H_7), 8.73 (s, 2H, $H_{6'}$), 8.59 (d, J = 3.0 Hz, 2H, $H_{7'}$), 8.37 (s, 2H, $H_{8'}$), 4.41 (m, 8H, H_4, $H_{4'}$), 3.22 (m, 2H, H_3), 2.32 (m, 2H, H_{1ax}), 1.80 (m, 2H, H_{1eq}), 1.60 (m, 2H, H_{2ax}), 1.23 (m, 2H, H_{2eq}).

Crystals of [La(tpzcn)I$_2$]I·0.5CH_3CN, **9**, suitable for X-ray diffraction studies were obtained from a 1:1 solution (1.4 × 10^{-2} M) of tpzcn and $LaI_3(thf)_4$ in acetonitrile left to stand at room temperature for few days.

[Ce(tpzcn)]. A solution of $CeI_3(thf)_4$ (81.0 mg, 0.100 mmol) in CH_3CN (5.0 mL) was added to a solution of tpzcn (48.3 mg, 0.100 mmol) in CH_3CN (5.0 mL). The resulting bright yellow solution was left to stand for 1 day. Bright yellow needles were then collected, washed with CH_3CN (2 × 2.0 mL), and dried under vacuum. Yield: 93% (93.4 mg).

Anal. Calcd for [Ce(tpzcn)I$_3$], $C_{26}H_{30}I_3N_{10}Ce$: C, 31.12; H, 3.01; N, 13.96. Found: C, 31.26; H, 3.19; N, 14.15.

Crystals of [Ce(tpzcn)I$_2$]I, **10**, suitable for X-ray diffraction studies were obtained from a 1:1 (0.7 × 10^{-2} M) solution of tpzcn and $CeI_3(thf)_4$ in acetonitrile left to stand at room temperature for few days.

Table 1. Crystallographic Data for the Six Structures of Complexes **1**−**6**

	tpztn, **1**	tpzcn, **2**	La(tpztn), **3**	La(tpztn), **4**	Ce(tpztn), **5**	Nd(tpztn), **6**
formula	$C_{23}H_{26}N_{10}$	$C_{26}H_{30}N_{10}$	$C_{23}H_{26}I_3LaN_{10}$	$C_{25.33}H_{29.50}I_3LaN_{11.17}$	$C_{25.33}H_{29.50}CeI_3N_{11.17}$	$C_{25.33}H_{29.50}NdI_3N_{11.17}$
fw	442.54	482.60	962.15	1010.04	1011.25	1015.37
cryst syst	triclinic	monoclinic	monoclinic	rhombohedral	rhombohedral	rhombohedral
space group	$P\bar{1}$	$C2$	$P2_1/n$	$R3c$	$R3c$	$R3c$
a, Å	9.3452(7)	22.9279(17)	17.6347(11)	33.6224(11)	33.5808(17)	33.4928(16)
b, Å	12.7195(9)	8.3801(6)	9.9451(6)	33.6224(11)	33.5808(17)	33.4928(16)
c, Å	19.694(1)	12.9290(1)	17.9814(11)	15.2549(7)	15.2125(11)	15.1242(10)
α, Å	99.973(1)	90.00	90.00	90.00	90.00	90.00
β, Å	98.952(1)	91.893(1)	110.9970(10)	90.00	90.00	90.00
γ, Å	91.910(1)	90.00	90	120.00	120.00	120.00
V, Å^3/Z	2273.1(3)/4	2482.8(3)/4	2944.2(3)/4	14 934.7(10)/18	14 856.4(15)/18	14 692.8(14)/18
l	0.710 73	0.710 73	0.710 73	0.710 73	0.710 73	0.710 73
D_{calc}, g cm^{-3}	1.293	1.291	2.171	2.021	2.035	2.066
μ(Mo Kα), mm^{-1}	0.084	0.083	4.628	4.112	4.219	4.462
temp, K	193(2)	298(2)	223(2)	193(2)	193(2)	223(2)
R_1, wR_2[a]	0.0668, 0.1768	0.0466, 0.1153	0.0404, 0.0925	0.0216, 0.0476	0.0286, 0.0647	0.0283, 0.0501

[a] Structure was refined on F_o^2 using all data: $wR_2 = [\sum[w(F_o^2 - F_c^2)^2]/\sum w(F_o^2)^2]^{1/2}$, where $w^{-1} = [\sum(F_o^2) + (aP)^2 + bP]$ and $P = [\max(F_o^2, 0) + 2F_c^2]/3$.

Table 2. Crystallographic Data for the Six Structures of Complexes **7**−**12**

	U(tpztn), **7**	Lu(tpztn), **8**	La(tpzcn), **9**	Ce(tpzcn), **10**	U(tpzcn), **11**	Nd(tpzcn), **12**
formula	$C_{25.33}H_{29.50}I_3N_{11.17}U$	$C_{29}H_{35}I_3LuN_{13}$	$C_{27}H_{31.50}I_3LaN_{10.50}$	$C_{27}H_{31.50}CeI_3N_{10.50}$	$C_{27}H3_{1.50}UI_1N_{10.50}$	$C_{27}H_{31.50}NdI_3N_{10.50}$
fw	1109.16	1121.37	1022.74	1023.95	1123.37	1028.07
cryst syst	rhombohedral	monoclinic	rhombohedral	rhombohedral	rhombohedral	rhombohedral
space group	$R3c$	$P2_1/n$	$R3c$	$R3c$	$R3c$	$R3c$
a, Å	33.4373(13)	10.262(3)	33.379(4)	33.281(3)	33.1530(12)	33.213(2)
b, Å	33.4373(13)	19.748(6)	33.379(4)	33.281(3)	33.1530(12)	33.213(2)
c, Å	15.1099(8)	18.636(6)	16.034(3)	16.032(3)	15.9643(8)	16.0155(18)
α, Å	90.00	90.00	90.00	90.00	90.00	90.00
β, Å	90.00	91.965(6)	90.00	90.00	90.00	90.00
γ, Å	120.00	90.00	120.00	120.00	120.00	120.00
V, Å^3/Z	14 630.3(11)/18	37 74.6(19)/4	15 471(4)/18	15 378(3)/18	15 195.9(11)/18	15 300(2)/18
l	0.710 73	0.710 73	0.710 73	0.710 73	0.710 73	0.710 73
D_{calc}, g cm^{-3}	2.266	1.973	1.976	1.990	2.210	2.008
μ(Mo Kα), mm^{-1}	7.876	5.108	3.970	4.076	7.584	4.285
temp, K	298(2)	193(2)	223(2)	193(2)	193(2)	223(2)
R_1, wR_2[a]	0.0306, 0.0705	0.0624, 0.1390	0.0350, 0.0672	0.0427, 0.0712	0.0420, 0.0881	0.0352, 0.0647

[a] Structure was refined on F_o^2 using all data: $wR_2 = [\sum[w(F_o^2 - F_c^2)^2]/\sum w(F_o^2)^2]^{1/2}$, where $w^{-1} = [\sum(F_o^2) + (aP)^2 + bP]$ and $P = [\max(F_o^2, 0) + 2F_c^2]/3$.

[U(tpzcn)I$_3$]. A green solution of $UI_3(thf)_4$ (28.2 mg, 0.311 mmol) in CH_3CN (1.0 mL) was added to a solution of tpzcn (15.0 mg, 0.311 mmol) in CH_3CN (2.0 mL). The resulting dark green solution was left to stand for 3 days. A dark green microcrystalline solid was then collected, washed with CH_3CN (2 × 1.0 mL), and dried under vacuum (1h). Yield: 55% (19 mg).

Anal. Calcd for [U(tpzcn)I$_3$], $C_{26}H_{30}I_3N_{10}U$: C, 28.35; H, 2.75; N, 12.72. Found: C, 28.11; H, 2.92; N, 12.50.

Crystals of [U(tpzcn)I$_2$]I, **11**, suitable for X-ray diffraction studies were obtained by slow diffusion at room temperature of a 0.7 × 10^{-2} M acetonitrile solution of tpzcn into a 0.7 × 10^{-2} M acetonitrile solution of $UI_3(thf)_4$.

[Nd(tpzcn)]. A solution of $NdI_3(thf)_{3.5}$ (67.4 mg, 0.083 mmol) in CH_3CN (2.0 mL) was added to a solution of tpzcn (40.0 mg, 0.083 mmol) in CH_3CN (2.0 mL). The resulting light green solution was left to stand for 1 day. A green crystalline solid was then collected, washed with CH_3CN (2 × 2.0 mL), and dried under vacuum. Yield: 93% (79.3 mg).

Anal. Calcd for [Nd(tpzcn)I$_2$]I·0.5CH_3CN, $C_{27}H_{31.5}I_3N_{10.5}Nd$: C, 31.54; H, 3.09; N 14.31. Found: C, 31.43; H, 3.29; N, 14.37.

Crystals of [Nd(tpzcn)I$_2$]I·0.5CH_3CN, **12**, suitable for X-ray diffraction studies were obtained from a 1:1 (1.4 × 10^{-2} M) solution of tpzcn and $NdI_3(thf)_{3.5}$ in acetonitrile left to stand at room temperature for few days.

X-ray Crystallography. All diffraction data were taken using a Bruker SMART CCD area detector three-circle diffractometer (Mo Kα radiation, graphite monochromator, λ = 0.710 73 Å). To prevent oxidation and/or hydrolysis, the crystals were coated with a light hydrocarbon oil and quickly transferred to a stream of cold nitrogen on the diffractometer.

The cell parameters were obtained with intensities detected on three batches of 15 frames. The crystal−detector distance was 5 cm. For three settings of Φ and 2Θ, narrow data frames were collected with 0.3° increments in ω. A full hemisphere of data was collected for **1**, **3**, **4**, **6**, **8**, and **11**, and a quadrant was collected for **2**, **5**, **7**, **9**, **10**, and **12**. At the end of data collection, the first 50 frames were recollected to establish that crystal decay had not taken place during the collection. Unique intensities with $I > 10\sigma(I)$ detected on all frames using the Bruker SMART program[36] were used to refine the values of the cell parameters. The substantial redundancy in data allows empirical absorption corrections to be applied using multiple measurements of equivalent reflections with the SADABS Bruker program.[36] Space groups were determined from systematic absences, and they were confirmed by the successful solution of the structure (Tables 1 and 2). Complete information on crystal data and data collection parameters is given in the Supporting Information.

The structures were solved by direct methods using the SHELXTL 6.10 package,[37] and all non-hydrogen atoms were found by difference Fourier syntheses. Hydrogen atoms for all compounds

(36) Bruker: Madison, WI, 1995.

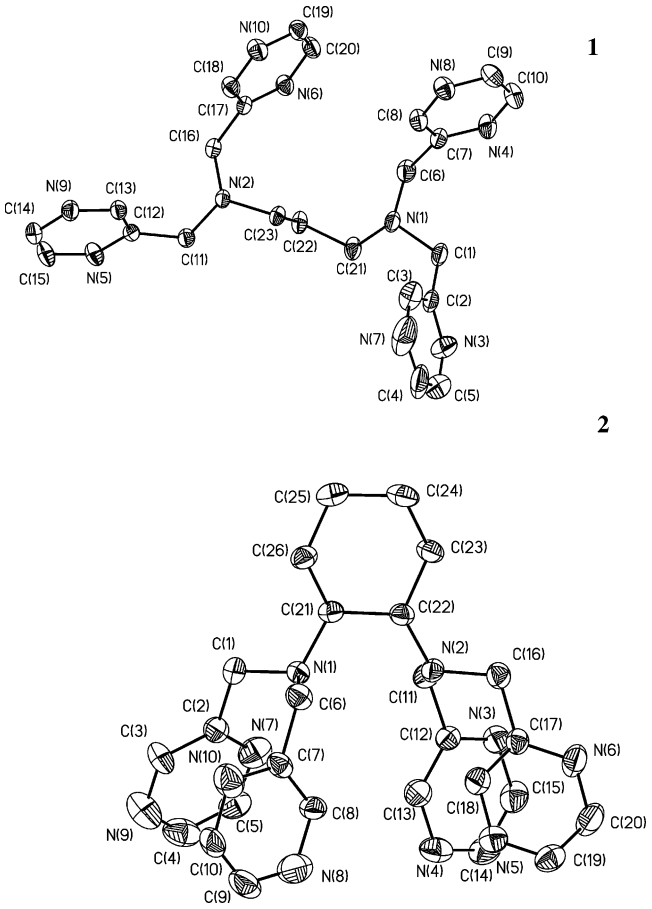

Figure 1. Molecular structure of the ligands tpztn (**1**) and tpzcn (**2**) with thermal ellipsoids at 30% probability.

were included in calculated positions and thermal parameters refined isotropically. All non-hydrogen atoms were anisotropically refined on F^2.

The comparison of M−N and M−O bond lengths in series of crystal structures of isostructural lanthanide complexes allowed us to estimate an uncertainty of ∼0.008 Å for the measured values of the M−N distances indicating that differences in bond distances larger than 0.025 Å are significant.

Results and Discussion

Synthesis and Characterization of the Ligands tpztn and tpzcn. The ligands were prepared by reacting under argon freshly prepared 2-(chloromethyl)pyrazine with trimethylenediamine or (±)-*trans*-1,2-diaminocyclohexane in the presence of K_2CO_3 and KI in anhydrous acetonitrile. The use of KI leads to a better yield in a shorter reaction time. After reflux (16 h) of the reaction mixture, purification of the crude product by flash chromatography, and recrystallization, the ligands were obtained as beige solids in 68−74% yield.

The ligands crystal structures were determined by X-ray diffraction studies. ORTEP diagrams of the molecular structure of tpztn (**1**) and tpzcn (**2**) are shown in Figure 1. In the structure of tpztn the two methylpyrazyl arms and the trimethylene bridge around each of the two aliphatic nitrogen

(37) Sheldrick, G. M. *SHELXTL 6.10*, 5th ed.; University of Göttingen: Göttingen, Germany, 1994.

Chart 2

atoms adopt the same helical conformation. The structure of tpzcn shows that the two aliphatic nitrogen atoms are preorganized for metal complexation because of the trans configuration of the cyclohexanediamine. The two methylpyrazyl arms around each of the two aliphatic nitrogens adopt a pincerlike conformation (Chart 2). The mean N−C (1.330(8) Å for tpztn and 1.34(2) Å for tpzcn) and C−C (1.37(1) Å for tpztn and 1.35(3) Å for tpzcn) distances of the pyrazine are similar to those found in free pyrazine.[38] The ^{1}H NMR spectrum of a solution of tpztn in CD_3CN indicates the presence of D_{2h} solution species in which all the pyrazyl arms are equivalent. The ^{1}H NMR spectrum of a solution of tpzcn in CD_3CN indicates the presence of C_2 solution species in which all the pyrazyl arms are equivalent. The methylene protons of the methylpyrazyl arms are diastereotopic (AB pattern). The lower symmetry of the tpzcn ligand and the diastereotopic character of the methylene protons arise from the trans configuration of the cyclohexanediamine spacer.

Formation of tpztn and tpzcn Complexes. [M(tpztn)I_3] complexes were prepared for M = La, Ce, Nd, Lu, and U by reacting tpztn with [MI_3(thf)$_4$] in anhydrous acetonitrile under argon. The complexes of Ce, Nd, and Lu are insoluble in acetonitrile and precipitate out of concentrate acetonitrile solution (85% yield).

The La(III) and U(III) complexes have a higher solubility in acetonitrile and can be isolated in 40−70% yield by adding diisopropyl ether.

[M(tpzcn)I_3] complexes were prepared for M = La, Ce, Nd, and U by reacting tpzcn with [MI_3(thf)$_4$] in anhydrous acetonitrile under argon. All complexes are highly insoluble and precipitate out of concentrate acetonitrile solutions (55−93% yield). Satisfactory elemental analyses were obtained for all complexes of tpztn and tpzcn.

The crystal structures of all complexes were determined by X-ray diffraction studies.

Crystal and Molecular Structure of [La(tpztn)I_3]. Two different types of crystals were obtained for the La complex of tpztn by slightly changing the crystallization conditions. The crystal structures of [La(tpztn)I_2]I, **3**, isolated from an acetonitrile/isopropyl ether solution, and [La(tpztn)I_2]I·1.17CH_3-CN, **4**, isolated from a concentrated acetonitrile solution, revealed two different geometric isomers of the cation [La(tpztn)I_2]$^+$. The ORTEP diagrams of [La(tpztn)I_2]$^+$ for **3** and **4** are shown in Figure 2. In both structures the La ion is

(38) Wheatley, P. *Acta Crystallogr.* **1957**, *10*, 182.

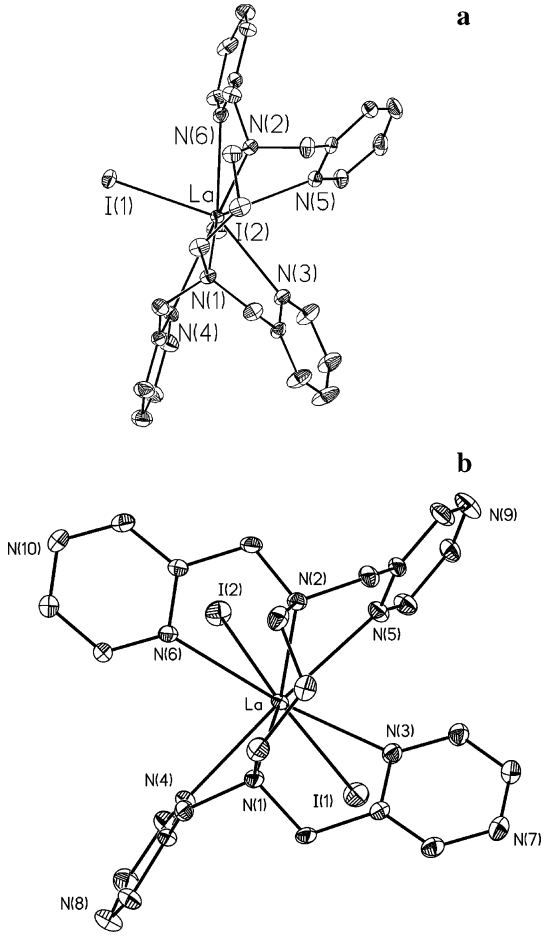

Figure 2. ORTEP diagram of the cation $[La(tpztn)I_2]^+$ in complex **3** (a) and in complex **4** (b), with thermal ellipsoids at 30% probability.

eight-coordinated by the six nitrogen atoms of tpztn acting as a hexadentate ligand and by two iodide ions. However, the ligand arms wrap around the metal center in two different ways. In the isomer **3** the methylpyrazyl arms adopt a double-pincer conformation (Chart 2) resulting in a coordination geometry which can be described as a distorted dodecahedron. In the isomer **4** the two methylpyrazyl arms and the trimethylene bridge around each aliphatic nitrogen adopt the same helical conformation resulting in a chiral molecule. The complex crystallizes as a racemic mixture of Λ,Λ and Δ,Δ enantiomers. The geometry around the metal ion is a distorted square antiprism with one square face formed by (I(1)N(3)N(1)N(4)) (deviation from plane: 0.09 Å) and the opposite face by (I(2)N(5)N(2)N(6)) (deviation from plane: 0.16 Å). The angle between the two faces is 9.4°. This is an additional example of the structural characterization of geometrical isomers for eight-coordinate complexes.[39,40]

The difference in the conformation adopted by the ligand arms leads to significant differences in the metal−ligand bond distances in the two geometric isomers with values of $La-N_{pyrazine}$ ranging from 2.680(3) to 2.794(3) Å in **3** and from 2.636(3) to 2.703(2) Å in **4** and with values of $La-N_{aliphatic}$ = 2.787(3) and 2.753(3) Å in **3** and 2.732(3) and 2.704(3) Å in **4**. Selected bond distances and angles of complex **3** are presented in Table 3, and selected bond distances of complex **4** are presented in Table 4. The mean value of $La-N_{pyrazine}$ in **3** is equal to the mean value found for the $La-N_{pyrazine}$ distances in the octacoordinated complex $[La(tpza)I_3(thf)]$ (2.74(5) Å) and is in the range of the La−N distances reported in the literature (2.79−2.60 Å). The mean value of $La-N_{pyrazine}$ in **4** is significantly shorter than in the tpza complex. The observed different values of bond distances in the two isomers can be rationalized in terms of a different strength of the metal−ligand interaction arising from the change in metal−ligand orientation. A better metal−ligand complementarity is likely to be achieved when the ligand adopts a double helical configuration than when it adopts a double pincer configuration.

Table 3. Selected Bond Lengths (Å) and Angles (deg) in Complex **3**

La−N(5)	2.731(3)	N(5)−La−N(2)	64.90(9)
La−N(4)	2.794(3)	N(4)−La−N(2)	141.99(10)
La−N(6)	2.759(3)	N(6)−La−N(2)	64.71(10)
La−N(3)	2.680(3)	N(3)−La−N(2)	104.74(10)
La−N(1)	2.787(3)	N(1)−La−N(2)	79.44(9)
La−N(2)	2.753(3)	N(5)−La−I(1)	139.41(6)
La−I(1)	3.1014(4)	N(4)−La−I(1)	85.98(7)
La−I(2)	3.1786(4)	N(6)−La−I(1)	79.49(7)
N(5)−La−N(4)	134.59(9)	N(3)−La−I(1)	141.39(8)
N(5)−La−N(6)	65.69(10)	N(1)−La−I(1)	81.27(7)
N(4)−La−N(6)	147.30(10)	N(2)−La−I(1)	82.11(7)
N(5)−La−N(3)	73.23(10)	N(5)−La−I(2)	84.67(7)
N(4)−La−N(3)	65.06(11)	N(4)−La−I(2)	78.47(7)
N(6)−La−N(3)	138.20(11)	N(6)−La−I(2)	78.99(7)
N(5)−La−N(1)	113.00(10)	N(3)−La−I(2)	90.14(8)
N(4)−La−N(1)	63.09(9)	N(1)−La−I(2)	139.57(6)
N(6)−La−N(1)	141.13(9)	N(2)−La−I(2)	139.49(7)
N(3)−La−N(1)	63.40(10)	I(1)−La−I(2)	109.339(11)

Crystal and Molecular Structures of $[Ln(tpztn)I_3]$ (Ce, Nd, Lu) and $[U(tpztn)I_3]$ Complexes. Crystals of the tpztn complexes of Ce, Nd, Lu, and U were obtained by letting stand at room temperature a concentrated 1:1 acetonitrile solution of tpztn and $[MI_3(thf)_x]$. The complexes $[Ce(tpztn)I_2]I\cdot 1.17CH_3CN$, **5**, $[Nd(tpztn)I_2]I\cdot 1.17CH_3CN$, **6**, and $[U(tpztn)I_2]I\cdot 1.17CH_3CN$, **7**, are isostructural with complex **4** with a square antiprism geometry of the eight-coordinate metal. The angle between the two faces of the distorted square antiprism with one square face formed by (I(1)N(3)N(1)N(4)) and the opposite face by (I(2)N(5)N(2)-N(6)) is 9.2° for U, 9.0° for Ce, and 8.4° for Nd (with similar deviation of the square faces from planarity for all complexes). A more important distortion from a regular square antiprism geometry is observed for the larger lanthanides. Selected bond distances and angles for complexes $[M(tpztn)I_3]$, **4**−**7**, are presented in Table 4. The Lu complex $[Lu(tpztn)(CH_3CN)_2]I_3\cdot CH_3CN$, **8**, shows a different coordination environment with respect to the lighter lanthanides. The ORTEP diagram of the cation $[Lu(tpztn)(CH_3CN)_2]^{3+}$ is shown in Figure 3, and selected bond distances and angles are presented in Table 5. The Lu ion is eight-coordinated by the hexadentate ligand tpztn and by two nitrogen atoms from two acetonitrile molecules with a slightly distorted

(39) Sen, A.; Chebolu, V.; Rheingold, A. L. *Inorg. Chem.* **1987**, *26*, 1821.
(40) Lippard, S. J. *Prog. Inorg. Chem.* **1967**, *8*, 109.

Table 4. Selected Bond Lengths (Å) and Angles (deg) in the [M(tpztn)I_3] Complexes **4**−**7** (Ir = Ionic Radius)

	La	U	Ce	Nd	ΔLa−U (Δir_{La-U} = 0.007)
M−N(5)	2.636(3)	2.593(3)	2.615(5)	2.578(5)	0.044
M−N(4)	2.667(3)	2.623(4)	2.641(5)	2.608(5)	0.047
M−N(6)	2.671(3)	2.630(3)	2.643(5)	2.620(5)	0.0404
M−N(3)	2.703(2)	2.665(4)	2.680(5)	2.654(4)	0.040
⟨M−N_{pyraz}⟩	2.669(27)	2.627(29)	2.645(27)	2.615(31)	0.042
M−N(2)	2.732(3)	2.698(3)	2.705(5)	2.671(4)	0.035
M−N(1)	2.704(3)	2.670(4)	2.678(5)	2.654(5)	0.033
M−I(1)	3.1643(4)	3.1408(3)	3.1447(5)	3.1212(5)	0.0237
M−I(2)	3.2089(3)	3.1805(4)	3.1901(5)	3.1647(5)	0.0284
N(5)−M−N(2)	64.07(11)	64.68(10)	64.74(16)	65.13(15)	
N(4)−M−N(2)	133.25(11)	134.18(10)	133.61(16)	134.73(15)	
N(6)−M−N(2)	62.03(11)	62.91(10)	62.35(15)	63.33(14)	
N(3)−M−N(2)	81.20(10)	81.40(11)	81.41(15)	81.67(14)	
N(1)−M−N(2)	81.68(10)	81.25(11)	81.97(15)	83.07(14)	
N(5)−M−I(1)	85.20(8)	84.88(8)	84.88(12)	84.55(11)	
N(4)−M−I(1)	79.88(8)	79.03(8)	79.48(12)	78.64(11)	
N(6)−M−I(1)	150.61(7)	149.94(8)	150.15(11)	149.19(11)	
N(3)−M−I(1)	74.12(8)	73.64(8)	73.85(11)	73.55(11)	
N(1)−M−I(1)	108.85(7)	108.18(7)	108.55(11)	107.81(11)	
N(2)−M−I(1)	144.69(7)	144.75(6)	144.95(10)	144.90(9)	
N(5)−M−I(2)	77.05(8)	76.75(8)	76.92(12)	76.51(11)	
N(4)−M−I(2)	91.63(8)	90.47(9)	90.32(12)	89.10(12)	
N(6)−M−I(2)	70.72(7)	70.63(8)	70.78(11)	70.54(10)	
N(3)−M−I(2)	148.06(7)	147.75(6)	147.66(11)	147.31(11)	
N(1)−M−I(2)	147.52(7)	147.25(7)	147.23(11)	147.00(10)	
N(2)−M−I(2)	100.68(7)	100.83(8)	101.05(11)	101.33(10)	
I(1)−M−I(2)	88.032(11)	88.168(9)	87.775(11)	87.435(15)	
N(5)−M−N(4)	161.59(12)	159.77(12)	160.20(17)	158.35(16)	
N(5)−M−N(6)	108.47(10)	109.52(11)	109.08(15)	109.72(15)	
N(4)−M−N(6)	80.66(10)	80.07(11)	80.12(16)	79.72(15)	
N(5)−M−N(3)	75.27(10)	75.32(11)	75.15(16)	75.43(15)	
N(4)−M−N(3)	110.43(11)	111.18(12)	111.48(16)	112.07(15)	
N(6)−M−N(3)	133.81(11)	134.66(11)	134.46(16)	135.58(15)	
N(5)−M−N(1)	130.38(11)	131.45(11)	131.26(16)	132.64(15)	
N(4)−M−N(1)	65.55(11)	66.19(12)	66.16(17)	66.51(16)	
N(6)−M−N(1)	82.47(10)	82.45(10)	82.46(15)	82.97(14)	
N(3)−M−N(1)	64.42(10)	64.96(10)	65.07(15)	65.56(15)	

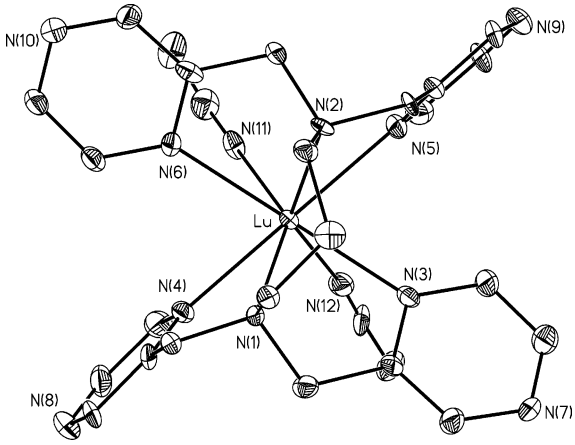

Figure 3. ORTEP diagram of the cation $[Lu(tpztn)I_2]^+$ in complex **8** with thermal ellipsoids at 30% probability.

square antiprism geometry. The angle between the two faces of the square antiprism with one square face formed by (N(12)N(3)N(1)N(4)) and the opposite face by (N(11)N(5)-N(2)N(6)) is 8.3°. The absence of coordinated iodide ions for Lu can be explained by an increased steric congestion around this smaller and more electropositive ion which prevents coordination of the large iodide ions. The higher tendency of lutetium iodide complexes to undergo ionization of the lanthanide−iodide bond has been recently reported.[41] The ligand adopts the same double helical conformation observed in the complexes [M(tpztn)I_3], **4**−**7**. The values of

Table 5. Selected Bond Lengths (Å) and Angles (deg) in $[Lu(tpztn)(CH_3CN)_2]^{3+}$, **8**

Lu−N(11)	2.377(9)	N(11)−Lu−N(5)	74.9(3)
Lu−N(12)	2.392(10)	N(12)−Lu−N(5)	78.1(3)
Lu−N(2)	2.439(8)	N(2)−Lu−N(5)	68.7(3)
Lu−N(4)	2.458(9)	N(4)−Lu−N(5)	147.2(3)
Lu−N(3)	2.463(9)	N(3)−Lu−N(5)	79.2(3)
Lu−N(5)	2.478(9)	N(11)−Lu−N(1)	143.5(3)
Lu−N(1)	2.480(8)	N(12)−Lu−N(1)	112.2(3)
Lu−N(6)	2.483(8)	N(2)−Lu−N(1)	86.2(3)
N(11)−Lu−N(12)	76.3(3)	N(4)−Lu−N(1)	68.6(3)
N(11)−Lu−N(2)	108.1(3)	N(3)−Lu−N(1)	69.9(3)
N(12)−Lu−N(2)	143.4(3)	N(5)−Lu−N(1)	140.9(3)
N(11)−Lu−N(4)	80.5(3)	N(11)−Lu−N(6)	71.2(3)
N(12)−Lu−N(4)	75.2(3)	N(12)−Lu−N(6)	142.3(3)
N(2)−Lu−N(4)	141.1(3)	N(2)−Lu−N(6)	67.3(3)
N(11)−Lu−N(3)	141.7(3)	N(4)−Lu−N(6)	80.9(3)
N(12)−Lu−N(3)	71.0(3)	N(3)−Lu−N(6)	145.6(3)
N(2)−Lu−N(3)	87.6(3)	N(5)−Lu−N(6)	110.4(3)
N(4)−Lu−N(3)	109.3(3)	N(1)−Lu−N(6)	84.8(3)

the M−N distances of the isostructural complexes [M(tpztn)-I_2]I (M = La, Ce, Nd, and U) are reported in Figure 4 as a function of the ionic radii of the metal ions.[42] They show a decrease from La to Ce and from La to Nd, which corresponds well to the decrease in ionic radius ($\Delta_{\langle M-Npyraz\rangle}$-La−Ce = 0.024 Å ($\Delta ir_{La-Ce}$ = 0.02 Å), $\Delta_{\langle M-Npyraz\rangle}$La−Nd = 0.054 Å ($\Delta ir_{La-Nd}$ = 0.05 Å)) as expected in a purely

(41) Giesbrecht, G. R.; Gordon, J. C.; Clark, D. L.; Scott, B. L. *Inorg. Chem.* **2004**, *43*, 1065.
(42) Shannon, R. D. *Acta Crystallogr.* **1976**, *A32*, 751.

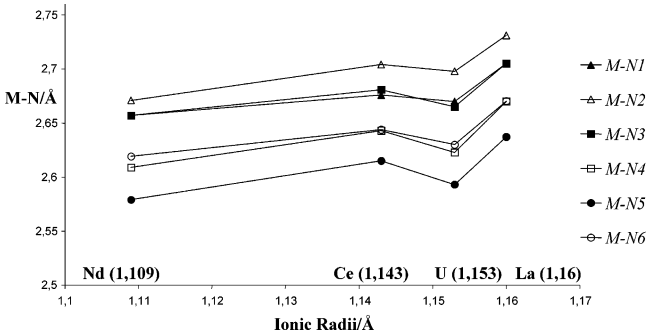

Figure 4. M−N bond lengths in the [M(tpztn)I_3], complexes as a function of the metal ionic radii.

ionic bonding model. Conversely the mean value of the $U-N_{pyrazine}$ distances is 0.042 Å shorter than the mean value of the $La-N_{pyrazine}$ distances, a difference significantly larger than the decrease expected from the variation of the ionic radii (0.007 Å[42]). This value is similar to the difference found between [U(tpza)(thf)I_3] and [La(tpza)(thf)I_3] complexes (0.046(3) Å) indicating the presence of a very similar metal−heterocyclic nitrogen interaction, despite the different geometrical arrangement of the pyrazyl groups.

As found for the tpza complexes,[10] no significant lengthening of the N−C or C−C bonds was observed in the [U(tpztn)I_3], complex with respect to the free ligand.

Crystal and Molecular Structures of [Ln(tpzcn)I_3] and [U(tpzcn)I_3] Complexes. Crystals of the tpzcn complexes of La, Ce, Nd, and U were obtained by letting stand at room temperature concentrated 1:1 acetonitrile solutions of tpzcn and [$MI_3(thf)_x$]. The complexes [La(tpzcn)I_2]I·0.5CH_3CN, **9**, [Ce(tpzcn)I_2]I·0.5CH_3CN, **10**, [Nd(tpzcn)I_2]I. 0.5CH_3CN, **11**, and [U(tpzcn)I_2]I·0.5CH_3CN, **12**, are isostructural with a square antiprism geometry of the eight-coordinate metal. The angle between the two faces of the distorted square antiprism with one square face formed by (I(1)N(6)N(2)N(5)) and the opposite face by (I(2)N(4)N(1)N(3)) is 15.7° for La, 15.0° for Ce, 15.3° for U, and 13.6° for Nd (with similar deviation of the square faces from planarity for all complexes). A more important distortion from a regular square antiprism geometry is observed for the larger lanthanides. The ORTEP diagram of the cation $[Ce(tpzcn)I_2]^+$ is shown in Figure 5, and selected bond distances and angles for the complexes [M(tpzcn)I_3], **9**−**12**, are presented in Table 6. The ligand tpzcn coordinates the metal ion in the complexes[M(tpzcn)I_3], **9**−**12**, in a fashion similar to that of the ligand tpztn in the complexes [M(tpztn)I_3], **4**−**7**. The two methylpyrazyl arms around each aliphatic nitrogen atom adopt the same helical conformation resulting in a chiral molecule. The complexes crystallize as a racemic mixture of Λ,Λ and Δ,Δ enantiomers. A significant $\pi\angle\pi$ interaction is observed in the complexes [M(tpzcn)I_3], between two essentially parallel pyrazine rings with a short separation between atoms C9 and C14. The mean values of the $M-N_{pyrazine}$ distances are similar to those found for the tpztn complexes. The values of the M−N distances for M = La, Ce, Nd, and U are reported in Figure 6 as a function of the ionic radii of the metal ions.[42] They show a decrease from La to Ce and from La to Nd, which corresponds well to the

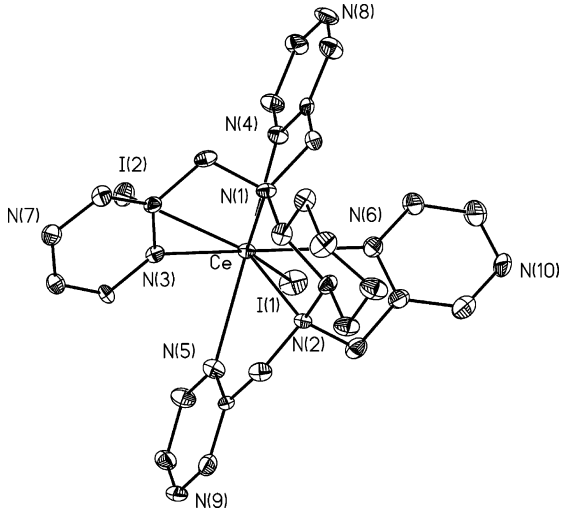

Figure 5. ORTEP diagram of the cation $[Ce(tpzcn)I_2]^+$ in complex **9** with thermal ellipsoids at 30% probability.

decrease in ionic radius ($\Delta_{\langle M-Npyraz\rangle}La-Ce = 0.031$ Å ($\Delta ir_{La-Ce} = 0.02$ Å), $\Delta_{\langle M-Npyraz.\rangle}La-Nd = 0.050$ Å ($\Delta ir_{La-Nd} = 0.05$ Å)) as expected in a purely ionic bonding model. As observed for the tpztn ligand, the differences in the values of the M−N distances between the uranium and the lanthanum complexes are significantly larger than the decrease expected from the variation of the ionic radii (0.007 Å[42]). The mean value of the distance $U-N_{pyrazine}$ is 0.054 Å shorter than the mean value of the $La-N_{pyrazine}$ distance. This value is similar to those found for the tpztn and the tpza complexes indicating the presence of a very similar metal−heterocyclic nitrogen interaction for the three ligands. Like in the tpza and tpztn complexes no significant lengthening of the N−C or C−C bonds was observed in the tpzcn complexes of uranium with respect to the free ligand. Likewise a significant lengthening of these distances was not observed in the structure of the $[Ru^{II}(NH_3)_5$ pyrazine$]^{2+}$ complex despite the presence of π back-bonding between Ru(II) and pyrazine.[43]

Solution Structure of the tpztn and tpzcn Complexes. For the tpztn complexes the characterization of the solution species was performed by NMR spectroscopy in acetonitrile. For the tpzcn complexes the characterization of the solution species by NMR spectroscopy was possible only for the lanthanum ion due to the low solubility of the Nd, Ce, and U complexes in organic solvents.

The proton NMR spectrum of a 1:1 solution of tpzcn and $LaI_3(thf)_4$ at 298 K in deuterated acetonitrile shows the presence of only one set of signals with six resonances for the pyrazine protons, two resonances for the diastereotopic methylene protons adjacent to the pyrazine, and five resonances for the protons of the cyclohexane moiety. These features are in agreement with the presence of C_2-symmetric solution species. The presence of two different sets of signals for the two methylpyrazine bound to the same aliphatic nitrogen atoms indicates that in solution the two aliphatic nitrogen atoms of the cyclohexanediamine spacer are bound to the lanthanum ion on the NMR time scale. The proton

(43) Gress, M. E.; Creutz, C.; Quicksall, C. *Inorg. Chem.* **1981**, *20*, 2.

Table 6. Selected Bond Lengths (Å) in the Complexes [M(tpzcn)I_3], **9**−**12** (Ir = Ionic Radius)

	La	Ce	Nd	U	ΔLa−U ($\Delta ir_{La-U} = 0.007$)	ΔLa−Ce ($\Delta ir_{La-Ce} = 0.02$)	ΔLa−Nd ($\Delta ir_{La-Nd} = 0.05$)
M−N(5)	2.646(8)	2.618(8)	2.601(9)	2.593(12)	0.053	0.028	0.045
M−N(4)	2.607(7)	2.577(7)	2.549(8)	2.537(11)	0.07	0.030	0.058
M−N(1)	2.708(7)	2.681(7)	2.649(8)	2.677(10)	0.049	0.027	0.045
M−N(2)	2.684(7)	2.653(7)	2.632(8)	2.627(10)	0.045	0.042	0.054
M−N(6)	2.734(8)	2.707(8)	2.689(9)	2.685(12)	0.031	0.027	0.059
M−N(3)	2.704(7)	2.662(7)	2.650(8)	2.659(11)	0.057	0.031	0.052
$\langle M-N_{pyraz}\rangle$	2.672(59)	2.641(56)	2.622(60)	2.618(66)	0.054	0.031	0.05
M−I(2)	3.2056(9)	3.1816(9)	3.1519(10)	3.1695(10)	0.036	0.020	0.0537
M−I(1)	3.1709(10)	3.1502(9)	3.1221(11)	3.1432(11)	0.0277	0.019	0.0488

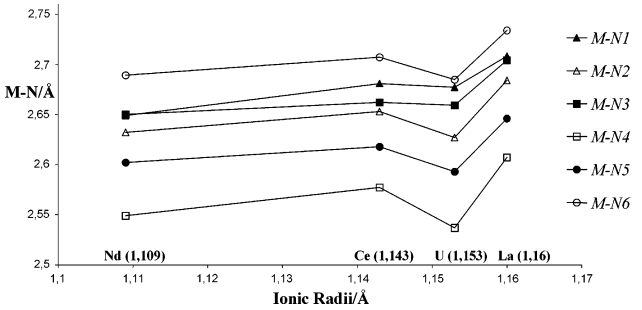

Figure 6. M−N bond lengths in the [M(tpzcn)I_3], **9**−**12**, complexes as a function of the metal ionic radii.

NMR of [La(tpzcn)I_3] remains unchanged in the temperature range 238−333 K suggesting the absence of exchange processes on the NMR time scale that could result in a dynamically averaged C_2-symmetrical structure. These features are in agreement with the presence of rigid solution species retaining the solid-state double helical conformation. The proton NMR spectra of the complexes of U, Nd, and Ce at 298 K show broad signals that could indicate the presence of exchange processes. The insolubility of these complexes prevented further characterization of the solution species by NMR spectroscopy.

The proton NMR spectrum of a 1:1 solution of tpztn and $LaI_3(thf)_4$ in deuterated acetonitrile at 298 K shows the presence of only one set of signals with three resonances for the pyrazine protons, two resonances for the diastereotopic methylene protons adjacent to the pyrazine, and two resonances for the methylene groups of the aliphatic chain. These features are in agreement with the presence of C_{2v}-symmetric solution species in which all methylpyrazine arms are equivalent. The proton NMR spectra of 1:1 solutions of tpztn and $MI_3(thf)_4$ (M = Ce, U, Nd) in deuterated acetonitrile at 298 K show broad signals in agreement with the presence of slow-exchange processes. At 333 K (or at 343 K for Ce) these processes become faster and the proton NMR spectra show only one set of seven sharper signals. The spectrum of the neodymium complex at 333 K is shown in Figure 7a. The spectral features of three resonances for the pyrazine protons, two resonances for the diastereotopic methylene protons adjacent to the pyrazine, and two resonances for the methylene groups of the aliphatic chain are in agreement with a dynamically averaged C_{2v}-symmetrical solution structure in which all methylpyrazine arms are equivalent.

The diastereotopic character of the methylene protons of the methylpyrazine arms in these complexes indicates that the two aliphatic nitrogen atoms remain bound to the metal ion on the NMR time scale. If the metal−$N_{aliphatic}$ bond is not labile, the quaternary nitrogen atom is indeed asymmetric as far as one methylpyrazyl group is concerned. The appearance of the protons of the methylene groups of the propylene bridge as singlets can be interpreted in terms of a short lifetime of the metal−$N_{pyrazine}$ bond (a long lifetime of this bond would give rise to multiple patterns for these protons). An interpretation of the spectral patterns in terms of bond labilities has been previously reported for lanthanide complexes of edta[44−46] and dota.[47] The spectrum of $[Lu(edta)]^-$ which shows a AB quartet pattern for the acetate protons and a singlet for the ethylenic protons was interpreted in terms of the presence of long metal−nitrogen and short metal−oxygen bond lifetimes.

However, the appearance of the methylene groups as singlets in the spectra of the tpztn complexes could also be interpreted in terms of averaging by exchanges between symmetry-related species which does not necessarily imply pyrazine decoordination. Such conformational exchange processes leading to signal averaging have been reported for the lanthanide complexes of the acyclic ligand dtpa (diethylenetriaminepentaacetate).[48]

To discriminate between the different possibilities we have performed proton NMR studies in the temperature range 238−343 K.

The proton NMR spectra of the La, Ce, and U complexes of tpztn at low temperature show broad signals indicating that an exchange process is slowed. The signals remain broad for La at the lowest temperature accessible in acetonitrile (238 K). For the uranium and the cerium complex at 238 K the exchange process is slowed significantly (a number of narrow signals larger than 9 can be observed), but some signals remain coalesced.

However, the proton NMR spectrum of the tpztn complex of neodymium in deuterated acetonitrile at 238 K shows 13 signals of equal intensity (Figure 7b) indicating the presence of rigid C_2-symmetric solution species with the C_2 axis passing through the carbon of the central methylene group of the trimethylene bridge and through the metal. The diastereotopic character of the methylene protons of the methylpyrazine arms and of the trimethylene bridge indicates

(44) Day, R. J.; Reilley, C. N. *Anal. Chem.* **1964**, *36*, 1073.
(45) Day, R. J.; Reilley, C. N. *Anal. Chem.* **1965**, *37*, 1326.
(46) Baisden, P. A.; Choppin, G. R.; Garrett, B. B. *Inorg. Chem.* **1977**, *16*, 1367.
(47) Desreux, J. F. *Inorg. Chem.* **1980**, *19*, 1319.
(48) Jenkins, B. G.; Lauffer, R. B. *Inorg. Chem.* **1988**, *27*, 4730.

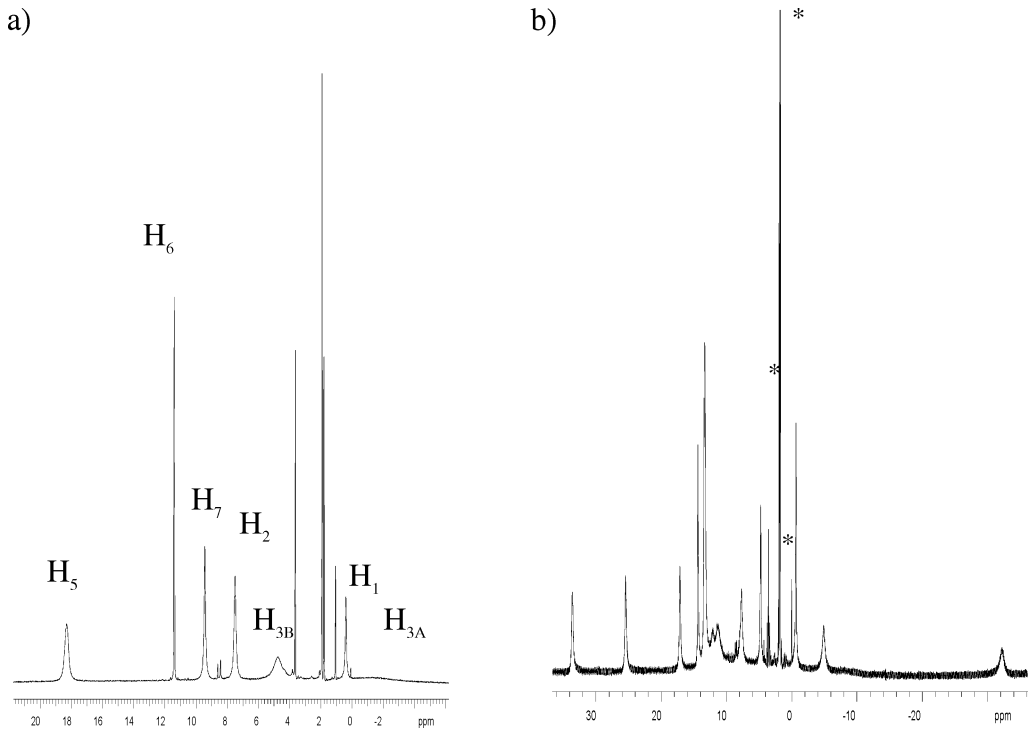

Figure 7. ^{1}H NMR (CD_3CN, 500 MHZ) of a 1:1 solution of tpztn (10^{-2} M) and $NdI_3(thf)_{3.5}$ at 333 K (a) and 238 K (b) (∗ = solvents).

that the two aliphatic nitrogen atoms and the four pyrazine nitrogen atoms remain bound to the metal ion at this temperature on the NMR time scale. The ^{1}H EXSY spectrum at 238 K shows six exchange peaks between 12 different protons. The peak (at −0.40 ppm) which is not involved in exchange can be assigned to the protons of the central methylene group. This spectral pattern suggests that the presence at 333 K of a C_{2v} symmetry of the solution species arises from exchange. The simple observed coalescence behavior is consistent with an exchange occurring between two C_2-symmetric double-helical enantiomers of the Nd complex and leading to an averaged C_{2v} symmetry. The crystal structure shows indeed a chiral double helical arrangement of the ligand. In the case of neodymium the NMR studies indicate that the six nitrogen atoms of the ligand remain bound to the metal in solution on the NMR time scale and that a conformational exchange occurs at room temperature which can be slowed at 238 K.

The different behavior of the solution species shown by the NMR spectra in the temperature range 238−343 K for La, Ce, and Nd could be explained by a higher kinetic inertness of the complexes of the smaller lanthanide due to a decreased flexibility. A similar improved kinetic inertness with small Ln(III) has been observed with other series of lanthanide podates.[48,49]

To further investigate this possibility we prepared and characterized the tpztn complex of lutetium. The proton NMR spectrum of a 1:1 solution of tpztn and $LuI_3(thf)_4$ in deuterated acetonitrile at 298 K shows the presence of a major C_{2v} symmetric species displaying seven broad signals and an additional minor solution species with lower symmetry. Further investigation of these species was prevented by the poor solubility of the lutetium complex. The NMR signals of the major species change in the temperature range 238−343 K and a simple coalescence behavior is observed which is consistent with the presence of an exchange occurring between two C_2-symmetric double-helical enantiomers leading to an averaged C_{2v} symmetry.

In conclusion, the proton NMR studies of the Nd(tpztn) and Lu(tpztn) complexes are consistent with the presence of solution species presenting rigid structures analogous to the solid-state structures where tpztn acts as an hexadentate ligand. Since kinetic inertness is expected to gradually increase going from large to smaller lanthanides, the nonrigid structure of the tptzn complexes of larger ions (La, Ce, U) in the studied range of temperatures could also be interpreted in terms of a similar faster C_2-C_{2v} exchange process. Although the presence of different exchange processes cannot be ruled out completely by the NMR studies for the larger ions, this interpretation is supported by the similarity of the solid state structures of the isolated compounds, which show for La, Ce, Nd, U, and Lu the same chiral double-helical arrangement of the ligand. Indeed only for the lanthanum compound an additional geometric isomer was isolated which could point to a different fluxional behavior for this ion.

These solution studies show that the double-helical arrangement adopted by these tetrapodal ligands in the solid state and leading to differences in bond lengths between uranium and lanthanides is retained in acetonitrile solution at least for some of the species studied.

Conclusion

In this paper we have described solid-state and solution-state structural studies of two rare examples of isostructural

(49) Renaud, F.; Piguet, C.; Bernardinelli, G.; Bünzli, J.-C. G.; Hopfgartner, G. *J. Am. Chem. Soc.* **1999**, *121*, 9326.

4f/5f pairs with ligands other than cyclopentadienyl derivatives, which allow a significant comparison of the metal−ligand interaction.

Despite the lack of selectivity observed for the ligands tpztn and tpzcn in the An/Ln separation, the crystallographic study on isostructural series of the tpzcn and tpztn complexes presented here shows, for both ligands, shorter $M-N_{pyrazine}$ distances in the uranium complexes with respect to the lanthanide ones. These differences can be interpreted in terms of a stronger $M-N_{pyrazine}$ interaction for uranium with respect to the lanthanide ions. The differences in the values of the $M-N_{pyrazine}$ distances are similar to those observed for the complexes of the tripodal ligand tpza which have been interpreted in terms of the presence of a uranium−pyrazine π back-bonding interaction. Theoretical density functional studies on model complexes corroborated this interpretation.

The results presented here show that the incorporation of pyrazyl nitrogens into a tetrapodal arrangement of tpztn and tpzcn can also lead to differences in the metal−nitrogen bond lengths between uranium and lanthanide ions. Therefore, the relationship between the differences in metal−nitrogen bond lengths and the selectivity in An(III)/Ln(III) extraction observed for tripodal and terdentate ligands is not evidenced for these tetrapodal ligands. This indicates that, besides the presence of donor atoms capable of establishing a back-bonding interaction, other parameters, such as the extractant geometry or the counterion, play an important role in the selectivity of ion recognition and need to be carefully considered in the design of selective extractants.

To investigate such parameters we are currently pursuing the structural study in solution and in the solid state of complexes of tetrapodal ligands with different geometries in the presence of different counterions.

Acknowledgment. This work was supported by the Commissariat à l'Energie Atomique, Direction de l'Energie Nucléaire.

Supporting Information Available: Complete tables of crystal and structure refinement data, atomic coordinates, bond lengths and angles, anisotropic displacement parameters, and hydrogen coordinates for compounds **1**−**12** in CIF format. This material is available free of charge via the Internet at http://pubs.acs.org.

IC049538M